Title: Functional connectivity reveals increased network segregation and sensorimotor processing during working memory in adolescents with Neurofibromatosis Type 1.

Authors: Marta Czime Litwińczuk[1], Nelson J Trujillo-Barreto[1,2,3], [Jeyoung Jung], Shruti Garg[1*], Caroline Lea-Carnall[1,3*]

Affiliations:

1. School of Health Sciences, University of Manchester, Manchester, UK
2. Geoffrey Jefferson Brain Research Centre, Manchester Academic Health Science Centre, Manchester, United Kingdom
3. School of Psychology, Manchester Metropolitan University, Manchester, UK

* these authors contributed equally to this work

Corresponding author: Marta Czime Litwińczuk
Corresponding author's email: marta.litwinczuk@manchester.ac.uk
Corresponding author's postal address: 3.316 Jean McFarlane, 176 Oxford Road, Manchester, M13 9PY, United Kingdom
Data/code availability: The NF1 participant data have been deposited on the Sage Bionetworks data repository https://www.synapse.org/. Approved researchers can request to obtain the data which are subject to data sharing agreements. Codes for data processing and analysis are available at https://github.com/MCLit/NF1-FC.
Ethics statement: Ethics approval for the study was obtained from the North West-Greater Manchester South Research Ethics Committee (reference: 18/NW/0762). Written informed consent was obtained from the parents and older adolescent participants and assent was obtained from the younger participants.
Conflict of Interests: None of the authors have a conflict of interest to disclose
Key words: neurofibromatosis, working memory, functional connectivity, graph theory

Acknowledgements: This research was supported by the NIHR Manchester Biomedical Research Centre (NIHR203308). ML was funded by the Office for Life Sciences and the National Institute for Health and Care Research (NIHR) Mental Health Translational Research Collaboration, hosted by the NIHR Oxford Health Biomedical Research Centre (NIHR203308). The views expressed are those of the author(s) and not necessarily those of the NIHR or the Department of Health and Social Care. The authors also wish to thank the NF1 participants and families that participated in this study. This work was also supported by the Neurofibromatosis Therapeutic Acceleration Program (NTAP) through a Francis Collins Scholarship to SG.

Abstract

Neurofibromatosis type 1 (NF1) is a rare genetic condition characterised by skin pigmentations, bone deformities, and tumours. . Its cognitive phenotype shares similarities with autism spectrum disorder and attention deficit/hyperactivity disorder, including

impairments in executive function and working memory processing.. In this work, we conducted functional connectivity and graph theory analysis of fMRI data from a sample of neurotypical adolescents (N = 26) and a sample of adolescent NF1 - participants (N = 43). Whole brain comparisons demonstrated that during working memory conditions NF1 participants have greater connectivity in left posterior parietal regions, particularly converging at the postcentral gyrus. Comparison of communication between functional networks demonstrated that NF1 participants have increased connectivity between visual, sensorimotor, dorsal attention and limbic networks. Individual connections were weaker in NF1 participants across the brain, and we found reduced connectivity between control, dorsal attention and default networks in NF1. Furthermore, connectivity strength in these networks (?) was predictive of accuracy and response time in NF1 participants during the task performance. Finally, graph theory analysis showed that working memory demands evoked reorganisation towards greater assortativity in NF1 participants, which was predictive of poorer accuracy and accuracy-speed trade-off. These findings highlight that NF1 participants' working memory deficits emerge from reduced engagement of executive processes, and NF1 participants demonstrate coping mechanisms such as enhanced sensorimotor processing and network reorganisation towards greater segregation, that is however detrimental to cognitive performance.

Introduction

Completion of everyday complex tasks requires encoding, storage and manipulation of information in our minds. This process known as working memory is essential for learning and decision making (Baddeley, 2012) and has been shown to impact learning and academic achievement (Swanson & Alloway, 2012). Many neurodevelopmental conditions have disrupted executive function, particularly working memory processes (Alloway et al., 2009; Martinussen et al., 2005; Wang et al., 2017). Neurofibromatosis type 1 (NF1) is one such neurodevelopmental disorder, with affects working memory processing speed and accuracy (Lehtonen et al., 2015b; Shilyansky et al., 2010). More specifically, NF1 participants show greater performance deterioration (i.e. slower responses, reduced accuracy) than controls when working memory increased (Shilyansky et al., 2010). NF1 is caused by mutation of the NF1 gene, that encodes the neurofibromin protein and regulates the Ras-MAPK molecular pathway (Daston & Ratner, 2005; North et al., 1997).

Previous studies used functional magnetic resonance imaging (fMRI) to elucidate the functional substrates of working memory in NF1 participants. For example, Shilyansky et al.

(2010) found that during performance of visuospatial working memory, NF1 participants show less activation dorsolateral prefrontal cortex, striatum, frontal eye fields, and parietal cortex than neurotypical controls. These regions are widely recognised to contribute to working memory in neurotypical groups (Owen et al., 2005), and Shilyansky's findings suggest an differences in recruitment of resources essential for working memory in NF1 groups. Ibrahim et al. (2017) focused on study how working memory affects functional activation and functional connectivity (FC), which reflects the temporal synchrony of the regions' blood-oxygen-level-dependent (BOLD) signal and implies communications during cognitive processing. Controls and NF1 participants completed fMRI scans during performance of visuospatial working memory. It was found that NF1 participants had less deactivation of the posterior cingulate cortex (PCC) and temporal regions. Further, NF1 participants had greater connectivity between visual cortices and both PCC and parietal regions, and greater connectivity between PCC and the cerebellum. The role of posterior cingulate cortex is widely debated (Leech & Smallwood, 2019), as it is often deactivated during task performance and active during rest along with other default network regions (Raichle et al., 2001), and its activity is generally associated with processing of internally generated thought (Mason et al., 2007) and is also associated with poorer attention to external stimuli (Eichele et al., 2008). As result, Ibrahim and colleagues considered whether their results may be explained by the "default network interference" hypothesis (Violante et al., 2012). According to this hypothesis, there is increased activation of the default network during task performance that may interfere with task performance.

Aberrant brain dynamics in NF1 have also been investigated with resting state fMRI, which capture brain activity in the absence of explicit cognitive demands. Tomson et al. (2015) investigated resting state FC and its underlying architecture, as summarised with graph theory measures. Specifically, Tomson and colleagues focused on the tendency of the network to form distinct modules in which nodes cluster and connect strongly together. Such modules are generally accepted to reflect the brain's capacity to conduct specialised processing, while paths connecting modules are believed to allow exchange and integration of processes. Tomson and colleagues found that NF1 participants, as compared to controls, have increased short-range but diminished long-range connectivity, weaker clustering and weaker connectivity within modules. This suggests that cognitive deficits in NF1 are related to disruptions to long-range communication in the functional network .

In this work, we will build on our previously published work which investigated the effects of non-invasive brain stimulation in NF1 adolescents (Garg et al., 2022). The aim of

the present work, however, is to compare whole brain FC between NF1 participants and neurotypical controls during low and high verbal working memory loads. To fulfil this goal, we will first compare FC during 0-back and 2-back conditions of the N-back task (Kirchner, 1958) between the two groups. This will be done at the level of individual connections and at the level of the recognised resting-state networks (RSN) (Thomas Yeo et al., 2011). We will examine the differences in network re-organisation related to the effect of working memory load (difference between conditions). We will relate the neural correlates to accuracy and response time during the 2-back task with predictive modelling, to determine which connections are reliably related to working memory performance. Finally, we implement graph theory analysis to understand what organisational properties of the network are favourable to performance of working memory, and whether differences are observed between groups. Based on prior research, we hypothesize that NF1 participants will have greater connectivity between the default and visual networks, and these differences will be related to processing speed and accuracy.

Methods

Participants

Table 1 includes demographics information for NF1 participants and neurotypical controls. The data used here includes and expands on the data from a previous study described in detail in Garg et al. (2022). In the original study, 28 adolescents, aged 11–17 years, with NF1 diagnosis were recruited. Additionally, 17 new adolescent participants with NF1 were recruited, resulting in a total sample size of 43.

Table 1. Demographic data of study participants (43 NF1 participants, 26 controls).

	Mean Age (STD)	Sex (M/F)
NF1 participants	14.77 (1.86)	22/21
Controls	14.2 (2.76)	12/14

NF1 participants

All recruitment was done via the Northern UK NF- National Institute of Health, with (i) diagnostic criteria [National Institutes of Health Consensus Development Conference. Neurofibromatosis conference statement. Arch. Neurol. 45, 575–578 (1988).] and/or molecular diagnosis of NF1; (ii) no history of intracranial pathology other than asymptomatic optic pathway or other asymptomatic and untreated NF1-associated white matter lesion or glioma; (iii) no history of epilepsy or any major mental illness; and (iv) no MRI contraindications. Participants on pre-existing medications such as stimulants, melatonin or

selective serotonin re-uptake inhibitors were not excluded from participation. The study was conducted in accordance with local ethics committee approval (Ethics reference: 18/NW/0762, ClinicalTrials.gov Identifier: NCT0499142. Registered 5th August 2021; retrospectively registered, https://clinicaltrials.gov/ct2/show/NCT04991428). All methods were carried out in accordance with relevant guidelines and regulations.

Neurotypical controls

Twenty-six adolescents with no diagnosis of NF1 were recruited.. Controls' age and sex were matched to the sample of NF1 participants.

Working memory task

The N-back task was used to assess working memory performance in the participants (Kirchner, 1958). Within the scanner, participants were presented with a sequence of black coloured letters on a white screen. The participants were instructed to respond only to the target by pressing a handheld button. During the 0-back condition, the participants responded when the letter 'X' was presented on the screen. During the 2-back condition, the participants responded when letter on the screen matched the letter 2 screens before. The stimuli were presented for 2500 milliseconds. Each session consisted of 6 blocks of 0-back condition and 6 blocks of 2-back condition, each block was 30 seconds long and consisted of 9 target stimuli. Accuracy was calculated separately for 0-back and 2-back conditions (correct hits + correct omissions/total responses). Response times (RT) were calculated only for time to correct response to target stimuli. Inverse efficiency score (IES) was calculated by dividing RT by accuracy as a measure of speed accuracy trade-off, in which lower scores are reflect better cognitive performance (faster response at lower accuracy cost) (Bruyer & Brysbaert, 2011).

MRI acquisition

Structural scanning was conducted using a Philips Achieva 3 T MRI scanner (Best, NL) equipped with a 32-channel head coil. First, 3D T1-weighted magnetic resonance images were obtained in the sagittal plane with a magnetization-prepared rapid acquisition gradient-echo sequence (repetition time = 8.4 ms; echo time = 3.77 ms; flip angle = 8°; inversion time = 1150 ms; in-plane resolution = 0.94 mm; 150 slices with 1 mm thickness). Next, a T2-weighted structural scan was performed using a turbo spin echo sequence (TR = 3756 ms; TE = 89 ms; 40 slices of 3 mm thickness and 1 mm gap; in-plane resolution = 0.45 mm).

Functional imaging was performed on a 3 Tesla Philips Achieva scanner using a 32-channel head coil with a SENSE factor 2.5. To maximise signal-to-noise (SNR), we utilised a dual-echo fMRI protocol developed by Halai et al. (2014). The fMRI sequence included 36 slices, 64×64 matrix, field of view (FOV) 224×126×224 mm, in-plane resolution 2.5×2.5 mm, slice thickness 3.5 mm, TR=2.5 s, TE = 12 ms and 35 ms. The total number of volumes collected for each fMRI session was 144.

fMRI Processing

Image processing was done using SPM12 (Wellcome Department of Imaging Neuroscience, London; http://www.fil.ion.ucl.ac.uk/spm) and MATLAB R2023a. Dual echo images were extracted and averaged using in-house MATLAB code developed by Halai et al. (2014) (DEToolbox). First, functional images were slice time corrected and realigned to first image. Then, the short and long echo times were averaged for each timepoint. The orientation and location of origin point of every anatomical T1 image was checked and corrected where needed. Mean functional EPI image was co-registered to the structural (T1) image. Motion parameters estimated during co-registration of short echo-time images were input to Artifact Detection Tools (ART; https://www.nitrc.org/projects/artifact_detect/) toolbox along with combined dual echo scans for identification of outlier and motion corrupted images across the complete scan. The outlier detection threshold was set to changes in global signal 3 z-scores away from mean global brain activation. Motion threshold for identifying scans to be censored was set to 3 mm. Outlier images and images corrupted by motion were censored during the analysis by using the outlier volume regressors. Participants with less than 80% of scans remaining were removed from analysis. Following the removal of participants with high motion and acquisition artefacts, 43 NF1 participants remained. Unified segmentation was conducted to identify grey matter, white matter, and cerebrospinal fluid. Normalisation to MNI space was done with diffeomorphic anatomical registration using exponentiated lie-algebra (DARTEL) (Ashburner, 2007) registration method for fMRI. Normalised images were interpolated to isotropic 2 × 2 × 2 mm voxel resolution. A 6x6x6mm full width at half maximum (FWHM) Gaussian smoothing kernel was applied.

Functional denoising was performed using the Conn toolbox (Whitfield-Gabrieli & Nieto-Castanon, 2012), we followed the default fMRI denoising pipeline (Nieto-Castanon, 2020). First, aCompCor removed confounding effects of signal from white matter and cerebrospinal areas, session and task effects, and subject-motion parameters (3 translation

and 3 rotation parameters) and global signal outlier scans, and session and task effects (Behzadi et al., 2007). Next, the denoising pipeline performed band-pass filtering (0.009–0.08 Hz) (Power et al., 2012; Yamashita et al., 2018). Functional connectivity was estimated for 356 regions of interest (ROIs) using 300 cortical parcels from Schaefer et al. (2018) (Schaefer-300) and 54 subcortical parcels from Automated Anatomical Labelling Atlas 3 (AAL3) Rolls et al. (2020). For each ROI, the timeseries of all voxels were extracted and averaged.

Average N-back task ROI-to-ROI functional connectivity (FC) was defined as Fisher-transformed Pearson's correlation coefficients (Fisher, 1915; Friston, 2011). In addition, condition-specific FC was estimated with weighted least squares linear model in which 0-back and 2-back boxcar timeseries were convolved with a canonical hemodynamic response function.

Whole brain FC analysis

To identify the how FC changes NF1 participants during N-back task, between 0-back and 2-back conditions, paired t-tests were performed for each connection in the whole brain FC. To determine if the differences in FC were statistically significant, 10,000 permutation tests were performed to generate null distribution of t-values. For each permutation, the signs of the direction of the difference in FC were randomly flipped across participants. The "max statistic" of the null distribution method was used for adjusting the p-values to control for family-wise error rates (FWER) (Groppe et al., 2011). The max-statistic of null distribution of t-values was compared against the observed distribution of t-values (p-value < 0.05). All the brain networks presented in this report were visualized with the BrainNet Viewer (http://www.nitrc.org/projects/bnv/) (Xia et al., 2013).

To aid interpretation of the results, those connections that show a significant effect of working memory were averaged for each seventeen cortical resting-state functional networks (Thomas Yeo et al., 2011) plus subcortical regions, resulting with a square, 18 by 18 adjacency matrix (RSN). This was done separately for positive and negative t-values.

Group comparisons

Permutation testing was employed to understand how 2-back condition and effect of working memory load (2-back>0-back) differs across NF1 participants and controls. For each permutation, the group labels were randomly shuffled (10,000 times), preserving the size of each group, and independent t-tests were repeated. The max-statistic of null distribution of t-

values was compared against the observed distribution of t-values (p-value < 0.05) (Groppe et al., 2011).

Graph theory analysis

Graph theory analysis was employed to understand the differences in organization of the networks across groups and conditions. First, spurious connections were masked out of the FC matrixes. Spurious connections were determined as those that have p-value > 0.05. P-values were calculated by dividing Fisher's Z scores by their corresponding standard errors to obtain Z-statistics, which were then converted to two-tailed p-values using the cumulative normal distribution. Pearson's correlation coefficients were obtained again. Negative connections were removed from the analysis. Then, five global graph theory measures (assortativity, global efficiency, modularity statistic, small world propensity, transitivity) were obtained for each condition using The Brain Connectivity Toolbox (http://www.brain-connectivity-toolbox.net). For small world propensity, the clustering coefficient was obtained using Onnela's algorithm and shortest path length was obtained using the Floyd–Warshall Algorithm (Muldoon et al., 2016; Onnela et al., 2005). Modularity statistic was estimated with Newman's algorithm (Newman, 2006).

Paired t-tests were performed for each group to assess if graph theory measures differed across 0-back and 2-back conditions. Independent t-tests were performed to compare if there were group differences in graph theory measures during either 0-back or 2-back condition.

Associations with behaviour

Connectivity

To assess how the connections that are significantly different between NF1 and control groups during 2-back condition are related to cognitive performance in the scanner, we fitted partial least squares (PLS) regression models. Models were separately fitted for NF1 participants and controls and for each group, models were separately fitted to accuracy and response time, resulting with 4 models in total.

We implemented cross-validation approach, dividing the sample into training and test samples. For both groups, 5 participants were selected for test samples, which makes 26% of controls sample and 12% of NF1 participant sample. During model training, we first performed an additional feature selection step to ensure model stability; for the training sample a leave-one-out correlation analysis was performed between connection strength and behavioural scores. This was repeated, leaving out one participant each time. Connections

that had significant correlation coefficients ($p < 0.05$) in at least 50% of the repeats were selected for model training. This ensured that we carried out model training using only those connections that were consistently related to behaviour. Next, we fitted PLS regression models with one component to predict behavioural outcomes. This process was repeated 100 times with random partitions of the data into training and test folds to ensure stability of the results. For illustration purposes, beta values were averaged across folds and repeats. Model generalizability was evaluated by averaging each participant's predicted scores across all repeats (obtained when they were in test sets) and calculating the coefficient of determination (R-squared) and Pearson's correlation coefficient between these averaged predictions and true scores.

To assess statistical significance of test sample predictions, we performed permutation testing by shuffling the behavioural scores and repeating the regression modelling with the connections used during model training. This was repeated 10,000 times, to generate a null-distribution of generalisability measures. Statistical significance was determined by comparing the true model's test sample coefficient of determination against the distribution of coefficients of determination obtained from the permutation testing.

Graph theory

To assess the generalisability of these results, we performed regression analysis with 10-fold cross-validation. First, confounding effects of demographics were regressed out of accuracy and IES. Then, linear regression was performed to predict these behavioural measures using network assortativity during the 2-back condition. Leave-one-out and 10-fold cross-validation were implemented to simulate population sampling. The predictive performance was measured using R-squared (R^2) and root mean square error (RMSE). Statistical significance was determined through permutation testing with 10,000 iterations. For each iteration, behavioural measures were shuffled, and the model was re-estimated on the training sample, then out-of-sample predictions were produced. P-values were computed as the proportion of permutations that yielded R^2 values greater than or equal to the observed R^2 values.

Results

Differences in performance on the N-back task

Figure 1 illustrates N-back performance of each group and effect of working memory on behavioural measures. There were no significant differences between NF1 participants and controls during 0-back condition in terms of accuracy ($t(61) = -0.31$, $p = 0.378$, $d = 0.08$),

response times ($t(61) = 1.65$, $p = 0.948$, $d = -0.45$) or IES ($t(61) = 1.15$, $p = 0.872$, $d = -0.31$). However, during the 2-back condition NF1 participants had significantly reduced accuracy as compared to controls ($t(61) = -3.00$, $p = 0.002$, $d = 0.81$). There were no significant differences in 2-back response times ($t(61) = 1.47$, $p = 0.927$, $d = -0.40$) or IES ($t(61) = 2.32$, $p = 0.988$, $d = -0.63$). In addition, compared to controls, NF1 participants exhibited a significantly greater decline in accuracy from 0-back to 2-back conditions ($t(61) = -2.27$, $p = 0.013$, $d = 0.62$), but not response times ($t(61) = 0.21$, $p = 0.582$, $d = -0.06$) or IES ($t(61) = 0.19$, $p = 0.574$, $d = -0.05$).

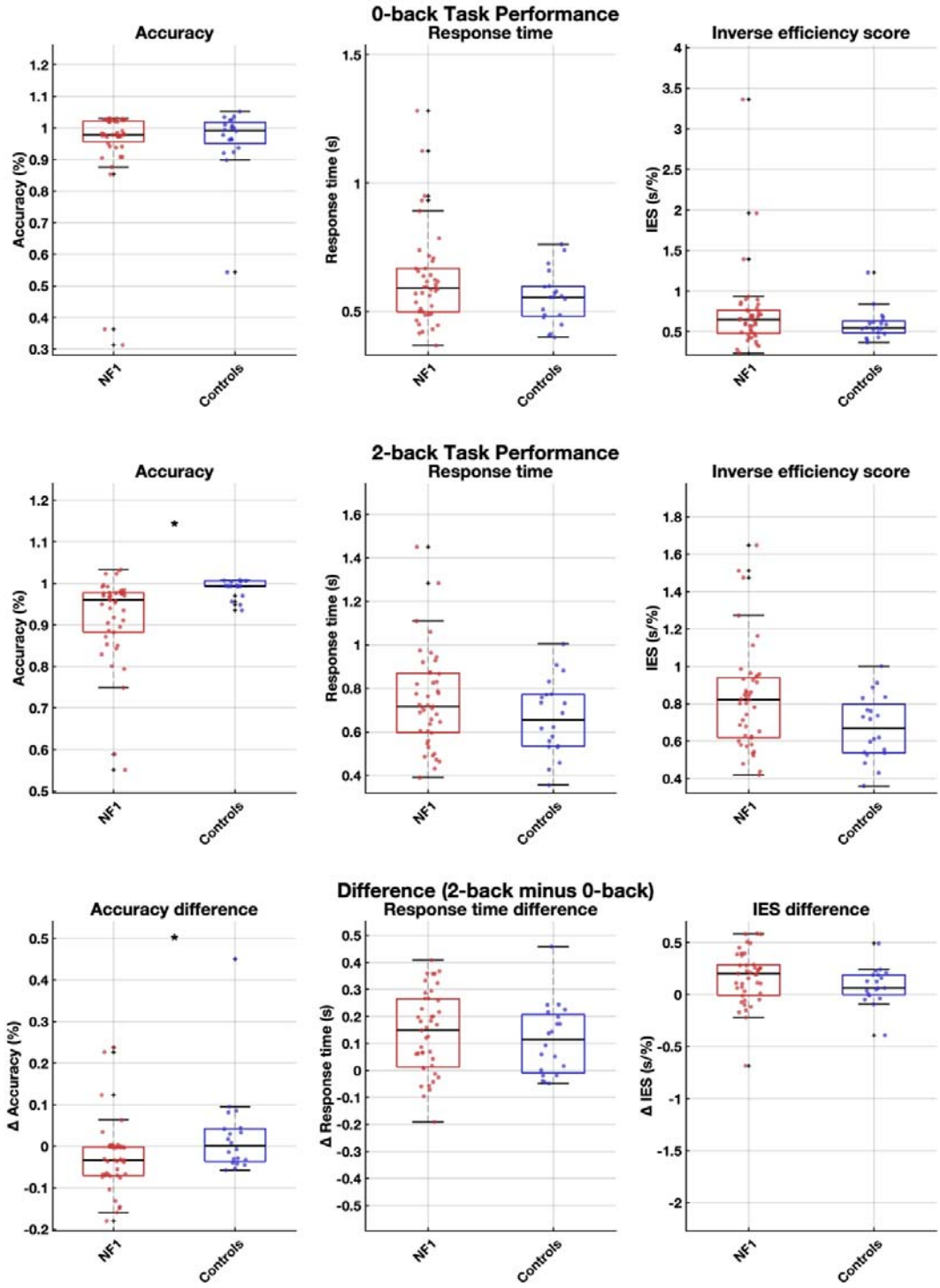

Figure 1 Boxplots illustrate NF1 participants' and controls' N-back task performance. The top and middle rows show raw performance on 0-back and 2-back conditions for accuracy, response time, and IES. The bottom row shows the difference in scores (2-back minus 0-back). Boxes represents the interquartile range (IQR) containing the middle 50% of the data, the horizontal lines inside indicate the median, the whiskers extend to the most extreme data not considered outlier. Individual dots represent individual participants' scores. Stars indicate significant differences between NF1 participants and controls. NF1 participants showed significantly reduced accuracy during 2-back condition and greater accuracy decline from 0-back to 2-back compared to controls.

Functional connectivity

Group differences during 2-back condition

Figure 2 illustrates whole brain FC differences between controls and NF1 group where red lines represent stronger connectivity during 2-back condition in NF1 participants and blue lines represent stronger connectivity during 2-back condition in controls. Supplementary Table [x] summarises all the connection pairs and their t-values (all passing the permuted probability alpha threshold of 0.001). NF1 participants had greater connectivity with left posterior regions, that converged in the left hemisphere for postcentral gyrus, precuneus, inferior parietal gyrus, superior parietal gyrus, and bilateral rolandic operculum. In contrast, NF1 participants had reduced connectivity throughout the frontal, parietal, temporal and occipital lobes and across hemispheres, highlighting brain-wide disruption during 2-back task.

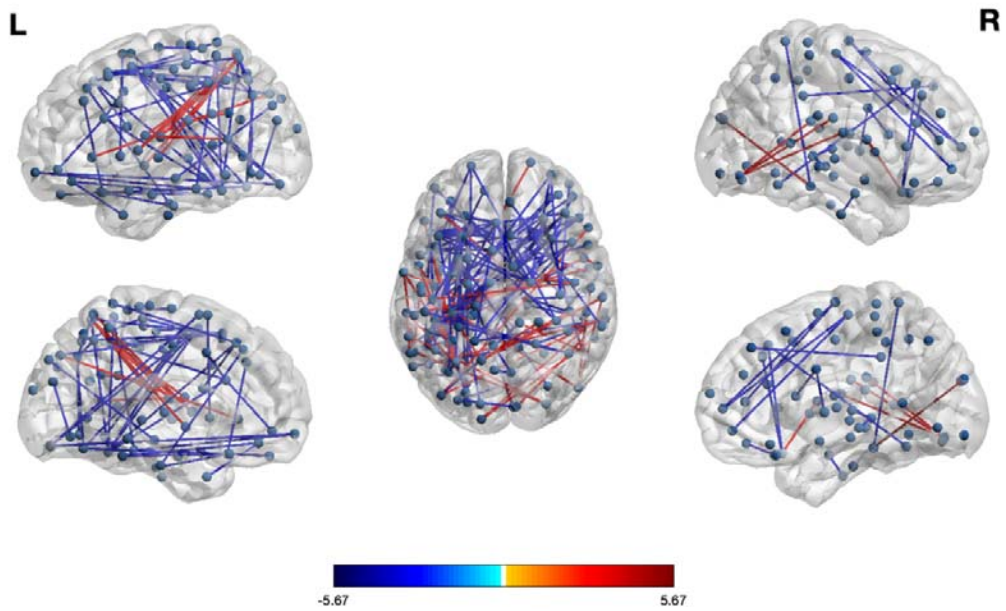

Figure 2 Whole brain FC differences between controls and NF1 participants during the 2-back condition. Red lines indicate stronger connections in NF1 participants, whereas blue lines indicate stronger connections in controls. Scale indicates t-values. All t-values have passed the probability threshold of 0.001 (permutation-corrected).

Association with behaviour

The PLS model significantly predicted accuracy during 2-back condition for both neurotypical controls and NF1 participants. Figure 3 and Figure 4 illustrate the connections that were predictive of accuracy in controls and NF1 participants, respectively.

For controls, accuracy was predicted in training sample with $R^2 = 0.556$ and in test sample with $R^2 = 0.046$ ($p_{permuted} < 0.045$). Better accuracy was found for those who had stronger connectivity between left Superior Frontal Gyrus and both right Fusiform Gyrus ($\beta = 0.019$) and right posterior Orbitofrontal Cortex ($\beta = 0.013$). In contrast, poorer accuracy was associated with stronger connectivity between right medial Orbitofrontal Cortex and left Fusiform Gyrus ($\beta = -0.018$), and between right middle Frontal Gyrus and left middle Cingulate Cortex ($\beta = -0.012$).

For NF1 participants, accuracy was predicted in training sample with $R^2 = 0.443$ and in test sample with $R^2 = 0.263$ ($p_{permuted} < 0.001$). For NF1 participants, accuracy was positively related to connection strength between the left superior frontal gyrus and both the left inferior parietal lobe ($\beta = 0.049$) and right fusiform gyrus ($\beta = 0.030$). Accuracy was also negatively related with frontal-frontal cross-hemispheric connectivity, where the strongest negative association was found between right superior frontal and left medial superior frontal regions ($\beta = -0.070$). In addition, negative associations with accuracy emerged for frontoparietal connectivity (left middle frontal gyrus with left lingual gyrus, $\beta = -0.048$; left middle frontal gyrus with right fusiform gyrus, $\beta = -0.057$) and for left-lateralised temporal-sensorimotor connectivity (middle temporal gyrus and rolandic operculum ($\beta = -0.055$), and between the middle temporal gyrus and postcentral gyrus ($\beta = -0.047$).

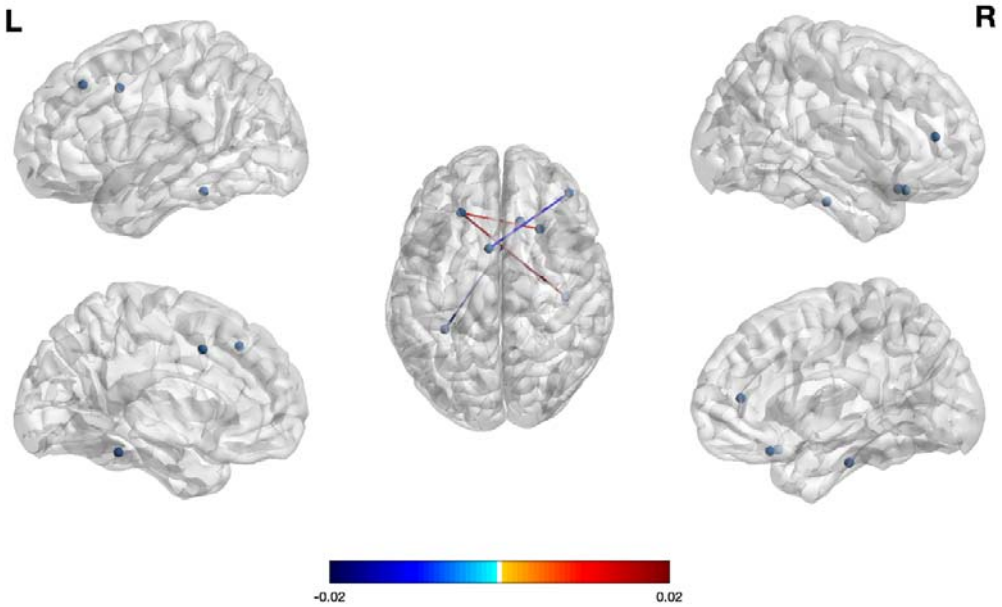

Figure 3 Brain networks predicting accuracy during 2-back condition in neurotypical controls. Red connections indicate that stronger functional connectivity is associated with better accuracy, while blue connections indicate that stronger connectivity is associated with poorer accuracy

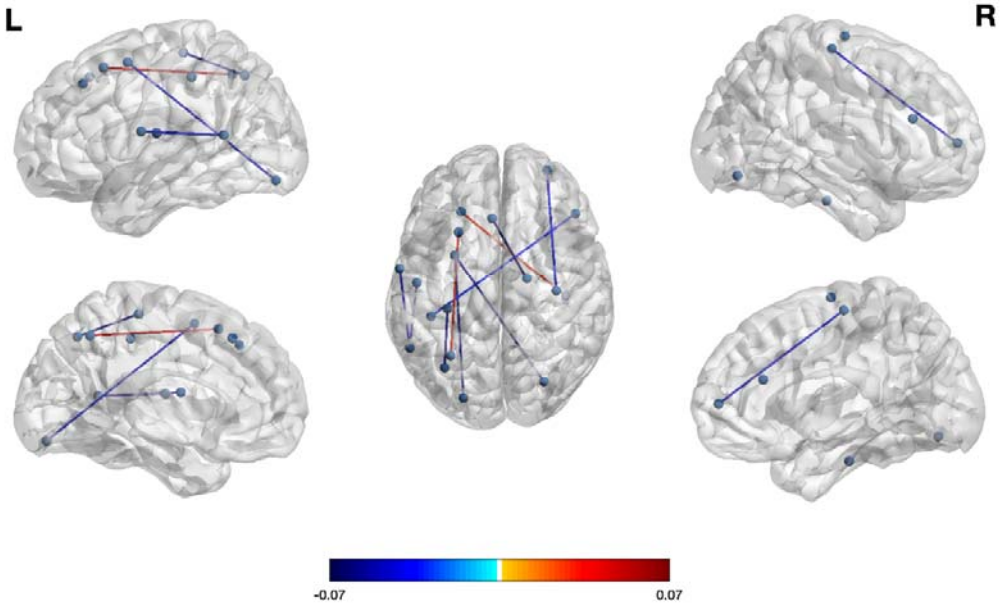

Figure 4 Brain networks predicting accuracy during 2-back condition in NF1 participants. Red connections indicate that stronger functional connectivity is associated with better accuracy, while blue connections indicate that stronger connectivity is associated with poorer accuracy.

Next, PLS model could not significantly predict response times during 2-back condition for neurotypical controls (training sample $R^2 = 0.482$; test sample $R^2 = 0.046$, $p_{permuted} = 0.071$). Response times in NF1 participants were also predicted by FC in training sample with $R^2 = 0.325$ and in test sample with $R^2 = 0.183$ ($p_{permuted} = 0.002$). Figure 5 illustrates the connections that were predictive of NF1 participant response time. NF1 participants were faster with stronger connectivity in parietal-sensorimotor and frontal-parietal networks (left Inferior Parietal Lobule and Postcentral Gyrus, $\beta = -0.116$; left Superior Frontal Gyrus and Superior Parietal Lobule, $\beta = -0.207$; and right Inferior Parietal Lobule and left Postcentral Gyrus, $\beta = -0.200$). However, stronger connectivity between right Inferior Occipital Gyrus and left Postcentral Gyrus was predictive of slower responses ($\beta = 0.213$).

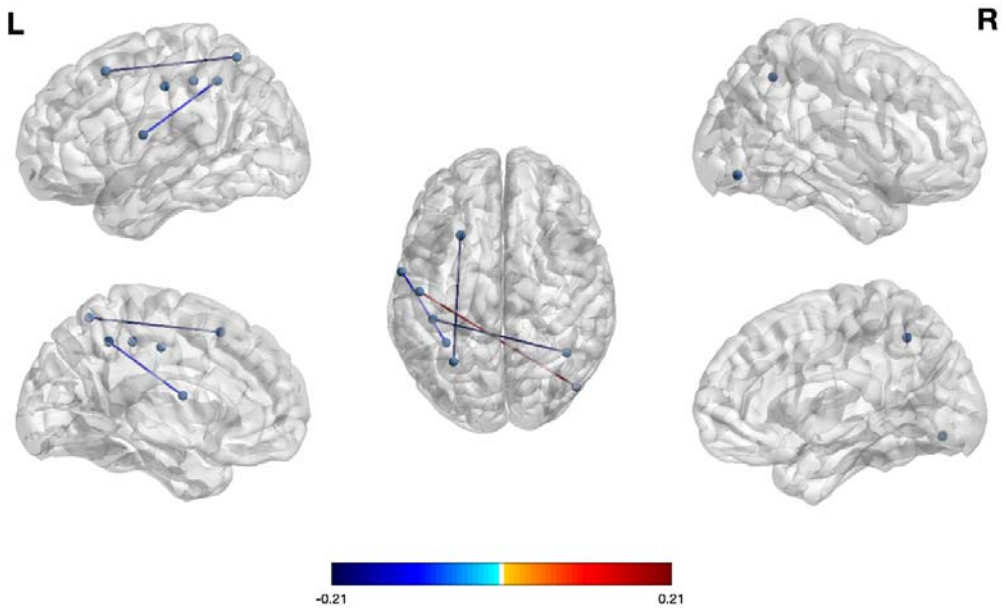

Figure 5 Brain networks predicting response time during 2-back condition in NF1 participants. Red connections indicate that stronger functional connectivity is associated with faster responses, while blue connections indicate that stronger connectivity is associated with slower responses.

Finally, PLS model could not significantly predict IES during 2-back condition for neurotypical controls (training sample $R^2 = 0.216$; test sample $R^2 = -0.036$, $p_{permuted} = 0.2$) or NF1 participants (training sample $R^2 = 0.250$; test sample $R^2 = -1.462$, $p_{permuted} = 0.796$).

Group differences in effect of working memory (2-back>0-back)

Figure 6 illustrates how change in FC from 0-back to 2-back conditions differed across NF1 participants and controls, where red lines represent more gain in FC in NF1

participants and blue lines represent more gain in FC in controls. Relative to controls, NF1 participants had atypical pattern of gain in FC from 0-back to 2-back for connectivity of left postcentral gyrus. Further, compared to controls, NF1 participants lacked gain in FC converging at the bilateral precentral and right postcentral gyrus, as well as bilateral middle frontal gyrus, left middle temporal gyrus, left inferior parietal gyrus and bilateral inferior frontal gyri.

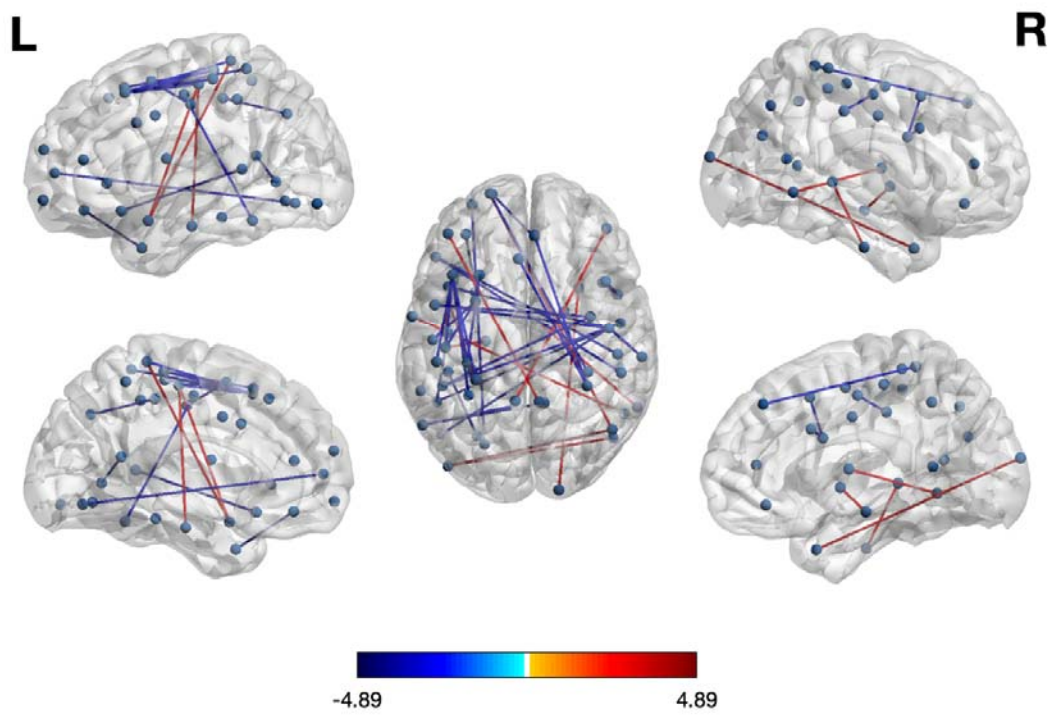

Figure 6 Brain network illustrates how effect of working memory (2-back>0-back) differed across NF1 participants and controls, where red lines represent more gain in FC in NF1 participants and blue lines represent more gain in FC in controls

Functional connectivity of Resting State Networks (RSN-FC)

Group differences during 2-back condition

Figure 7 illustrates group differences in RSN-FC during 2-back condition. It was found that NF1 participants relied more on communication between central visual (composed of striate and extrastriate cortex) and somatomotor B networks (composed of primary and secondary sensorimotor cortex, insula and auditory cortex) (t = 2.260, p = .027), somatomotor B and limbic B networks (composed of orbital frontal cortex) (t = 2.116, p = .041), somatomotor B and limbic A networks (composed of temporal pole) (t = 2.052, p = .043), somatomotor B and dorsal attention A networks (composed of temporal occipital

cortex, parietal occipital cortex, and superior parietal lobule) (t = 2.007, *p* = .049). However, NF1 participants relied less on connectivity between subcortical and temporal parietal (composed of temporoparietal cortex) (t = -3.919, *p* < .001), limbic B with itself (t = -3.756, *p* < .001), somatomotor A and control B (composed of temporal lobe, inferior parietal lobule, dorsal prefrontal cortex, lateral prefrontal cortex, lateral ventral prefrontal cortex, medial posterior prefrontal cortex) (t = -3.071, *p* = .002).

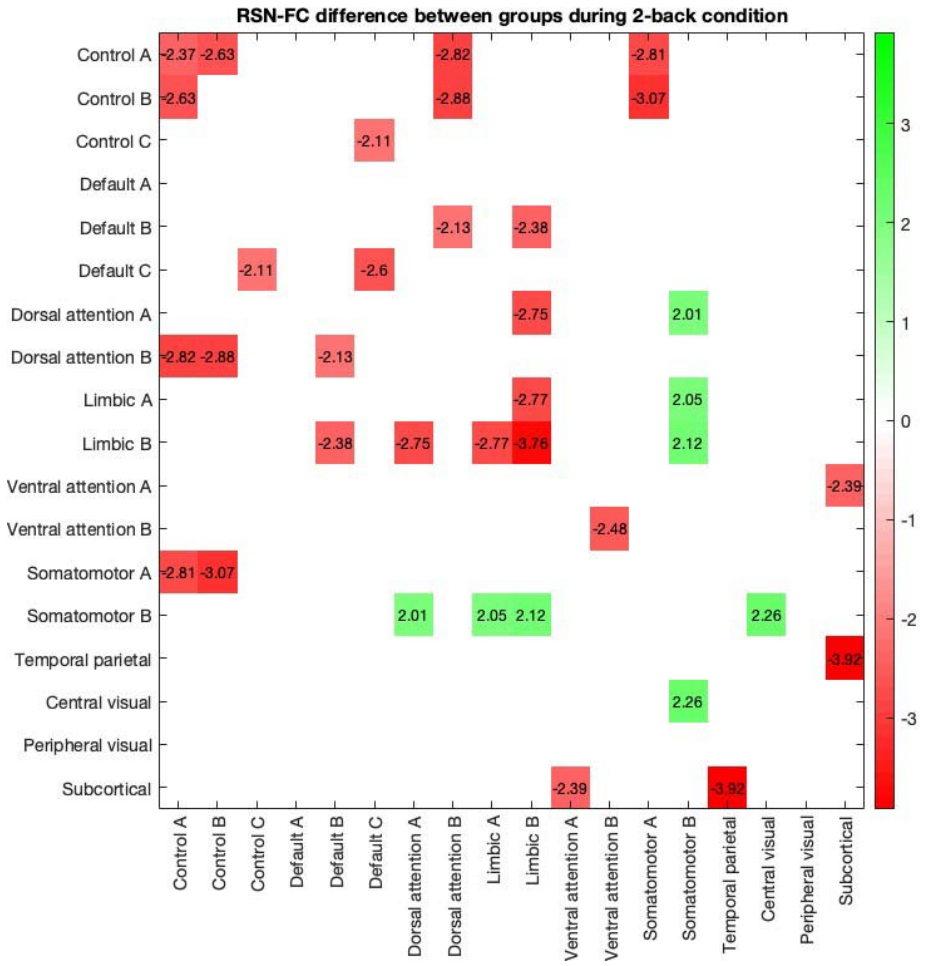

Figure 7 Group differences between NF1 participants and controls in RSN-FC during 2-back condition. Values in the heatmap represent t-statistics. Green values indicate stronger connectivity for NF1 participants and red values indicate weaker connectivity in NF1 participants. T-statistics with probability > 0.05, estimated with permutation testing, were masked out.

Group differences in effect of working memory (2-back>0-back)

Figure 8 illustrates group differences the effect of working memory on RSN-FC. As result of working memory, NF1 participants had weakened RSN-FC strength between control B (composed of temporal lobe, inferior parietal lobule, dorsal prefrontal cortex, lateral prefrontal cortex, lateral ventral prefrontal cortex, medial posterior prefrontal cortex) and dorsal attention B (composed of temporal occipital, post central, frontal eye fields, precentral

ventral) (t = -3.099, *p* = .003) and between default B (composed of temporal lobe, anterior temporal, dorsal prefrontal cortex, ventral prefrontal cortex) and dorsal attention B (t = -2.507, *p* = .015), but strengthened RSN-FC strength between default A (composed of temporal lobe, inferior parietal lobule, dorsal prefrontal cortex, precuneus posterior cingulate cortex, medial prefrontal cortex) and limbic B (composed of orbital frontal cortex) (t = 2.167, *p* = .031) in NF1 participants compared to controls.

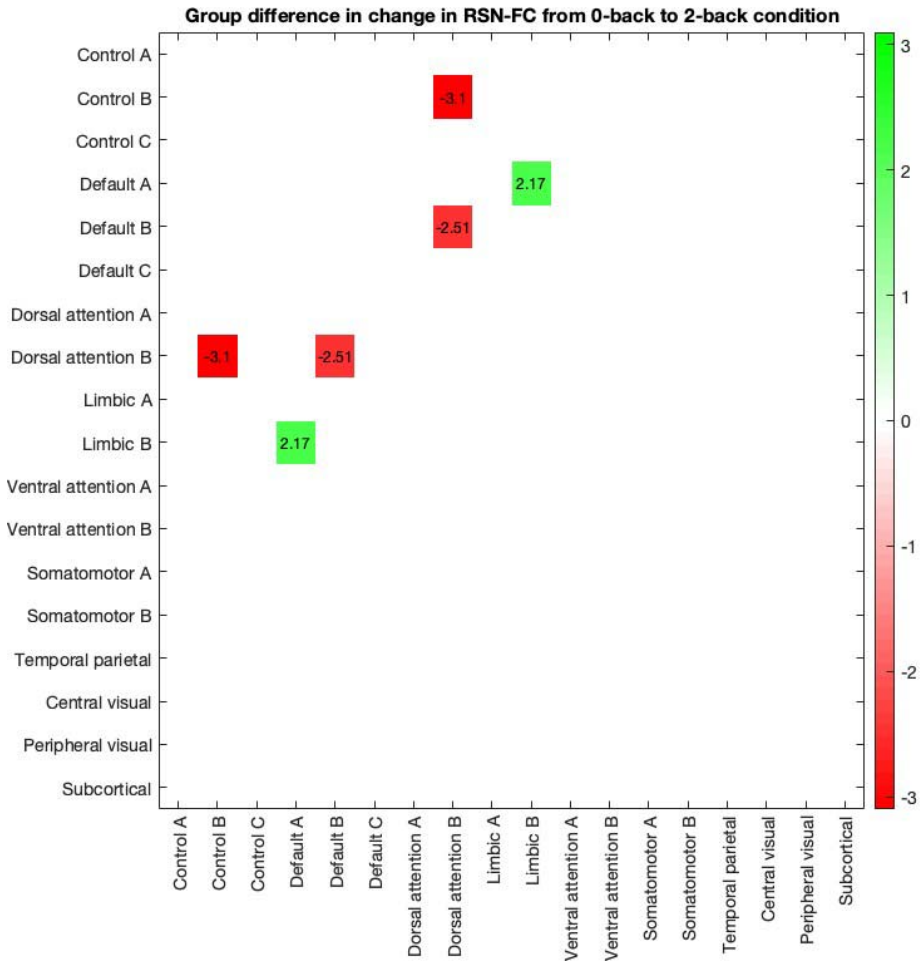

Figure 8 Group differences between NF1 participants and controls in effects of working memory (2-back>0-back) on RSN-FC. Values in the heatmap represent t-statistics. Green values indicate stronger connectivity for NF1 participants and red values indicate weaker connectivity in NF1 participants. T-statistics with probability > 0.05, estimated with permutation testing, were masked out.

Graph theory

Neurotypical controls had no condition-specific changes in any graph theory measures (small world propensity: t(18) = -0.457, p = 0.653; global efficiency: t(18) = -0.387, p = 0.703; assortativity: t(18) = 0.371, p = 0.715; modularity: t(18) = 0.059, p = 0.953; transitivity: t(18) = -0.443, p = 0.663). In contrast, in response to increased working memory

demands NF1 participants had increased assortativity (t(42) = 2.305, p = 0.026), but not small world propensity (t(42) = -0.799, p = 0.429), efficiency (t(42) = -1.179, p = 0.245), modularity statistic (t(42) = -1.386, p = 0.173) or transitivity (t(42) = -0.431, p = 0.668).

Comparison of graph theory measures obtained for 0-back and 2-back conditions revealed no significant differences between groups for either 0-back condition (small world propensity: t(60) = -1.111, p = 0.271; global efficiency: t(60) = -1.386, p = 0.171; assortativity: t(60) = 1.675, p = 0.099; modularity: t(60) = -0.305, p = 0.761; transitivity: t(60) = -0.427, p = 0.671) or 2-back condition (small world propensity: t(60) = -1.165, p = 0.249; global efficiency: t(60) = -1.664, p = 0.101; assortativity: t(60) = 0.992, p = 0.325; modularity: t(60) = 0.549, p = 0.585; transitivity: t(60) = -0.629, p = 0.532).

For the control sample, correlation analysis revealed that assortativity during 0-back task was negatively correlated with accuracy. During 2-back task, global efficiency had a positive correlation with response time and IES, such that poorer performance (longer response times and higher IES) was associated with higher global efficiency. In contrast, modularity showed negative correlations with both response time and IES, such that better performance was associated with higher modularity.

For the NF1 participant sample, correlation analysis revealed that assortativity during 2-back task correlated with NF1 participant accuracy and IES, such that poorer performance was associated with greater assortativity. Table 1 and Table 2 summarise all correlation analysis that have been ran for each group and during each condition.

Table 1 Results of correlation analysis in the control sample between global graph theory measures and behavioural outcomes during each condition. Confounding effects of demographics have been regressed out of the behavioural responses. Values outside the brackets present Pearson's R correlation coefficients, values inside the brackets present probability values generated with permutation testing. Bold font has been used to highlight significant correlations (alpha level 0.05, FWER-corrected with permutation testing)

	Accuracy	Response time	IES
0-back			
Small world propensity	0.05 (0.868)	0.11 (0.645)	0.05 (0.845)
Global efficiency	0.14 (0.396)	0.22 (0.378)	0.11 (0.625)
Assortativity	**-0.44 (0.045)**	0.07 (0.770)	0.23 (0.344)
Modularity	0.10 (0.655)	-0.20 (0.427)	-0.20 (0.391)

Transitivity	-0.02 (0.936)	0.23 (0.349)	0.17 (0.459)
2-back			
Small world propensity	0.18 (0.444)	0.28 (0.237)	0.28 (0.254)
Global efficiency	0.19 (0.426)	**0.58 (0.007)**	**0.58 (0.009)**
Assortativity	0.23 (0.335)	0.03 (0.904)	0.03 (0.905)
Modularity	-0.11 (0.688)	**-0.47 (0.042)**	**-0.47 (0.045)**
Transitivity	0.16 (0.498)	0.34 (0.140)	0.34 (0.157)

Table 2 Results of correlation analysis in the NF1 participant sample between global graph theory measures and behavioural outcomes during each condition. Confounding effects of demographics have been regressed out of the behavioural responses. Values outside the brackets present Pearson's R correlation coefficients, values inside the brackets present probability values generated with permutation testing. Bold font has been used to highlight significant correlations (alpha level 0.05, FWER-corrected with permutation testing)

	Accuracy	Response time	IES
0-back			
Small world propensity	-0.05 (0.743)	0.16 (0.313)	0.11 (0.474)
Global efficiency	-0.14 (0.362)	0.23 (0.133)	0.24 (0.128)
Assortativity	-0.26 (0.094)	0.01 (0.943)	0.15 (0.336)
Modularity	-0.00 (0.983)	-0.08 (0.603)	-0.09 (0.580)
Transitivity	-0.17 (0.286)	0.13 (0.396)	0.18 (0.238)
2-back			
Small world propensity	-0.14 (0.389)	-0.18 (0.251)	-0.09 (0.562)
Global efficiency	-0.14 (0.385)	0.01 (0.973)	0.05 (0.736)
Assortativity	**-0.47 (0.001)**	0.22 (0.155)	**0.40 (0.011)**
Modularity	0.05 (0.720)	-0.14 (0.354)	-0.13 (0.373)
Transitivity	-0.21 (0.177)	-0.03 (0.828)	0.06 (0.693)

Leave-one-out cross-validation revealed that network assortativity during 2-back condition could significantly predict NF1 participants' accuracy ($R^2 = 0.114$, RMSE = 0.096,

$p_{permutation}$ = 0.003) and IES (R^2 = 0.069, RMSE = 0.265, $p_{permutation}$ = 0.009) (Figure 9). Similar results were observed with 10-fold cross-validation, where network assortativity during the 2-back condition significantly predicted accuracy (R^2 = 0.071, RMSE = 0.098, $p_{permutation}$ = 0.007) and IES (R^2 = 0.110, RMSE = 0.259, $p_{permutation}$ = p = 0.001).

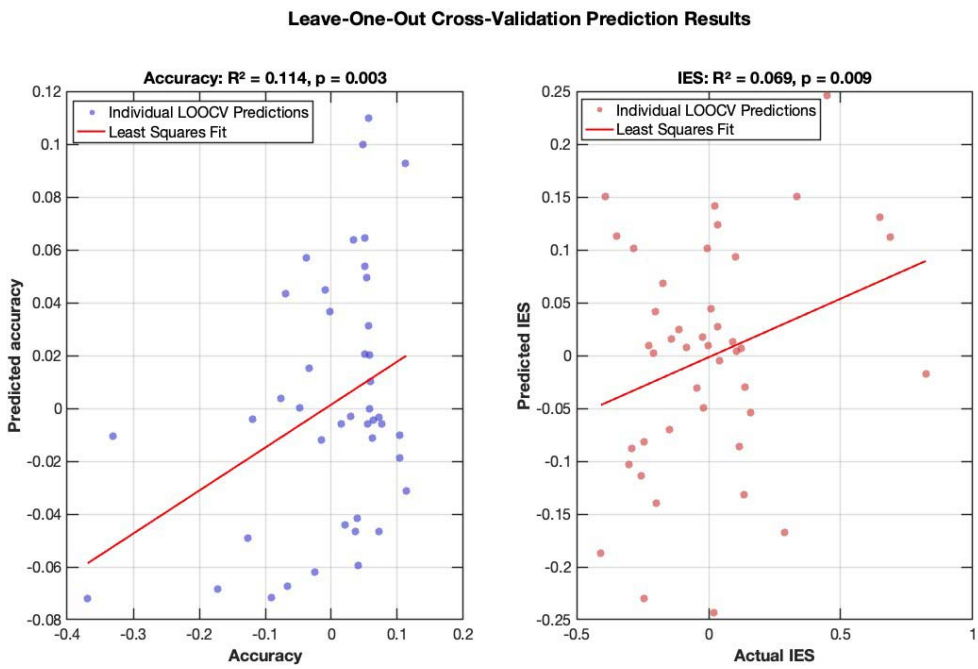

Figure 9 Results of leave-one-out cross-validation, using 2-back network assortativity to predict accuracy and IES.

Discussion

To our knowledge, this is the largest sample to investigate how the NF1 condition affects the functional networks during high and low working memory demands of the verbal N-back task. By analysing individual edges of FC, we demonstrated that during working memory NF1 participants have greater connectivity than neurotypical controls with left parietal regions, particularly post-central gyrus. We hypothesized that NF1 participants would have greater connectivity between default mode and visual networks than neurotypical controls. We investigated this hypothesis by averaging connectivity within and between widely recognised RSNs (Thomas Yeo et al., 2011) and comparing it across groups. Through this analysis we identified that in response to increasing working memory demands (2-back>0-back), relative to controls, NF1 participants had weakened connectivity between parts of default mode and dorsal attention networks but strengthened connectivity between default mode and limbic networks. This finding adds nuance to the default mode interference

hypothesis, as it suggests that NF1 participants have atypical adaptation of default mode network's communication with other network due to working memory demands, specifically reflecting asynchrony with higher-order networks. We further used graph theory measures to characterize network topology, and we found that high working memory demand led to increased assortativity for NF1 participants, which is characteristic of greater network segregation. This change was disruptive for NF1 participants' accuracy and speed-accuracy trade-off. Collectively, these findings suggest that NF1 is associated with changes to organisation of the functional brain networks during verbal working memory, such as increased regional connectivity, reduced connectivity with higher order networks associated with poorer accuracy and speed-accuracy trade-off. In this discussion we consider the implications of the findings from FC, RSN-FC and finally graph theory analysis as well as considering the future directions for this work.

Connectivity between individual regions (FC)

The FC results showed that during the 2-back condition, NF1 participants had stronger connectivity with left parietal regions, particularly postcentral gyrus, precuneus, inferior parietal gyrus, superior parietal gyrus, and bilateral rolandic operculum. In contrast to prior research, we found no evidence of enhanced engagement of posterior cingulate cortex (Ibrahim et al., 2017). This inconsistency may be related to the reduced visual and enhanced verbal processing needed during this version of the task. Instead, we found that NF1 participants had markedly greater connectedness with left postcentral gyrus. Postcentral gyrus constitutes part of the sensorimotor network (Thomas Yeo et al., 2011), and it is essential for motor control and preparation of motor responses (Alahmadi, 2024; Mastria et al., 2023). A greater motor response readiness does not explain this pattern, however, because this connectivity pattern did not appear for 0-back condition and instead it appeared to be working memory dependent. Therefore, the greater reliance on sensorimotor integration (via postcentral gyrus) during verbal working memory could reflect reduced engagement with core working memory related processes, or additional recruitment of neural resources to functionally compensate for any weakness in typical working memory processes or for any weakness in working memory network (such as indirect connectivity). Previous research suggests a variety of working memory strategies, such as subvocal phonological sound rehearsal strategy (Paulesu et al., 1993), visual pattern processing strategy (Pearson & Keogh, 2019) and motor/action-oriented strategy (Langner et al., 2014). Some evidence points that

postcentral gyrus may be involved in consolidation of verbal working memory (Mainy et al., 2007) possibly reflecting subvocalization (Fox et al., 1987; Perry et al., 1999). In particular, Marvel et al. (2019) suggest some motor regions support working memory by offering additional neuronal connections that can be used to increase signal-to-noise ratio, resulting with increased information maintenance and reduced loss of information by distractor stimuli. Therefore, imagined motor response (i.e. motor traces), such as traces of speech, may support working memory rehearsal in NF1 participants, and thus this difference in connectivity likely reflects a coping mechanism. Future work should explore whether multi-modal or hands-on learning approaches that take advantage of this processing difference could aid learning through engagement of sensorimotor processes. This could have profound impact on the support provided to NF1 participants in classrooms, aid development of personalized cognitive therapies (via enhanced engagement of motor-based learning and processing) and could potentially result with improved learning and quality of life. Motor function focused educational support approaches (e.g. rhythm focused learning, embodied learning, use of multi-sensory/manipulative learning tools) have already been explored in other neurodevelopmental conditions such as autism spectrum disorder and attention deficit/hyperactivity disorder (Chan et al., 2022) resulting with improved attention (Chan et al., 2022; Ding et al., 2024; Srinivasan et al., 2016) social communication but also benefit executive function typically developing children (Kosmas et al., 2018; Richter et al., 2024; Tomporowski et al., 2007).

A widespread network of connections was weaker in NF1 participants, and these patterns were predictive of behavioural outcomes. NF1 participants were more accurate when they had stronger connectivity between the left superior frontal gyrus and both the left inferior parietal lobe and right fusiform gyrus. The superior frontal gyrus is known for executive control and working memory maintenance (Boisgueheneuc et al., 2006), while inferior parietal regions support verbal working memory maintenance (Ravizza et al., 2004; Todd & Marois, 2004) and fusiform regions modulate visual inputs (Courtney et al., 1997; Grill-Spector et al., 2001). Put together, this suggests that NF1 participant accuracy relies on effective encoding and maintenance of inputs in working memory. In contrast, connectivity of middle frontal gyrus with regions related to visual processing (fusiform, lingual) was predictive of poorer accuracy. The middle frontal gyrus plays a key role in working memory manipulation and executive control (Mohr et al., 2006; Nee et al., 2013), with its connectivity to visual processing likely reflecting competition between manipulation and visual processing

or interruption of novel inputs (Grill-Spector et al., 2001). NF1 participants' responses were predicted by stronger connectivity between inferior parietal and postcentral gyrus – which suggests importance of sensorimotor connections with parietal regions for producing promptly motor responses during working memory task (Martuzzi et al., 2014). Further, fast responses were predicted by connectivity between superior frontal gyrus and superior parietal gyrus, which suggests benefit from top-down executive control (Boisgueheneuc et al., 2006; Corbetta & Shulman, 2002). The strength of these connections was compromised in NF1 participants. The only left connection that was stronger and associated with faster response times was the connection from left occipital to right postcentral gyrus, which suggests likely speed of visual inputs to the regions responsible for processing of motor responses (Simmonds et al., 2007).

Connectivity between resting state networks (RSN-FC)

Similar patterns were observed at the level of communication between various networks (RSN-FC). Through investigation of connections between networks, we found that NF1 participants have greater connectivity between visual, sensorimotor, dorsal attention and limbic networks. This further suggests that NF1 participants may rely more on motor integration strategies. RSN-FC analysis also illuminated patterns of weaker connectivity – it was found that NF1 participants had reduced connectivity between higher order networks as reflected by reduced connectivity between control, dorsal attention and default networks. The reduced connectivity between control and dorsal attention networks suggests reduced goal-driven attention, cognitive control for adaptive responses, task maintenance and switching (Cole & Schneider, 2007; Corbetta & Shulman, 2002; Dosenbach et al., 2007). Meanwhile, default mode network's affected regions include temporal and prefrontal regions, known for contribution to memory integration and executive processing (Simons & Spiers, 2003). Additionally, there was reduced connectivity between subcortical and temporoparietal regions, which may suggest poorer integration of bottom-up and top-down processing, such as input processing and goal-driven action that may be reflected by atypical gating of novel inputs into working memory storage (Corbetta & Shulman, 2002; Frank et al., 2001; McNab & Klingberg, 2007).

Importantly, these findings of RSN-FC further add nuance to the default mode interference hypothesis (Violante et al., 2013); increasing working memory demands was associated in patients with weakened connectivity between parts of default mode and dorsal

attention networks and increased connectivity between default and limbic networks. Prior research suggests that in response to cognitively demanding tasks our dorsal attention network would increase activity while the default mode network would decrease activity (Fox et al., 2005). Specifically, reports from clinical and neurotypical populations point that maintenance of activity in default mode network is associated with attentional lapses and many clinical populations have difficulty in suppressing default mode network's activity (Anticevic et al., 2012). Ibrahim et al. (2017) and Violante et al. (2013) raised the possibility that this difficulty to suppress the default mode network activity disrupts completion of visual and higher order tasks. When investigating this hypothesis, here we observed weakened connectivity between dorsal attention and default mode networks, which suggests greater segregation of their respective processes during higher working memory demands. The dorsal attention network is in part responsible top-down control processes, such as attentional selection and response preparation (Corbetta & Shulman, 2002). Therefore, it is possible that weakened connectivity between the dorsal attention and default mode networks suggests enhanced top-down control of processes associated with rest. This may mean that patients engage more effortfully with suppression or desynchronisation of default mode network's activity. At first, this may appear to contrast with the default mode interference hypothesis but we also observed increased connectivity between default mode and limbic network. This may reflect disrupted ability to switch engagement with various networks in response to changing working memory demands (Uddin, 2014), which is consistent with the default mode interference hypothesis. Additionally, the limbic network and parts of the default mode network such as posterior cingulate cortex are known to modulate the salience of internal and external stimuli (Leech & Smallwood, 2019; Seeley et al., 2007), suggesting possibility that the connectivity of default mode network to limbic regions is a coping mechanism that is modulating processing of novel representations and those stored previously.

To summarise, based on the present findings, we suggest that the connectivity of default mode network points towards reduced top-down processing (e.g. goal-driven attention, cognitive control for adaptive responses, task maintenance and switching) and increased engagement with modulation of processing of salient internal-external stimuli and atypical gating of novel stimuli to working memory.

Graph theory measures of network architecture

Finally, we explored whether specific organisational properties of FC are favourable to working memory performance and whether NF1 participants show disruptions to these properties. It was found that controls have no notable reorganisation of the network in response to increasing working memory demands but tend to perform better with more modular organization. For NF1 participants, modularity was not related to behavioural outcomes. However, working memory evoked network reorganisation in the NF1 participant group; NF1 participants had higher assortativity during 2-back condition, as compared to 0-back. Assortativity reflects the tendency of nodes with similar degrees to connect to each other. Therefore, in response to working memory demands, NF1 participants' network became more segregated. These comparative with the findings of Tomson et al. (2015), who found reduced anterior-posterior connectivity in NF1 participants during rest, as high assortativity may emerge from more segregated and more local processing. This change was predictive of poorer accuracy and poorer speed-accuracy trade-off (IES) during working memory performance. This suggests that the reorganisation in NF1 participants is not optimal for working memory performance, potentially due to increased segregation of processes and resulting difficulty in transfer of information through the network and difficulty in integration of processes. Previous work investigating FC during N-back in healthy young adults similarly demonstrates working memory performance is related to integrative, between-network communication (Cohen & D'Esposito, 2016; Shine et al., 2016; Spadone et al., 2015). Therefore, the segregation we observed in the NF1 sample related to working memory hinder cognitive performance.

Limitations and research avenues

This work has been the first to explore how working memory impacts whole-brain FC, network communication and graph theory measures in NF1 participants, and related these findings to behaviour with predictive modelling, demonstrating generalisability of the results. However, there are several key limitations that must be considered with this work. First, and foremost we focused on verbal working memory but cannot make any comments about many cognitive domains that are also challenging for NF1 participants, such as inhibitory control, task switching, language processing (Lehtonen et al., 2015a). As such it is not clear if the results of this work are generalisable to other high-demand cognitive tasks. Regarding the methodology, it is important to note that it focused on testing of individual connections independently of each other. This method can effectively identify strong

connection differences across conditions and groups, but it may miss small differences that span cross multiple connections. This was acceptable in the context of this work as we also explored communication between networks, and particularly as we took a similar approach to relate connectivity differences to behavioural outcomes. Methods such as network based statistics may be desired for studies focused on connected components that show disruption within the network (Zalesky et al., 2010).

Conclusions

In conclusion, this work has highlighted notable differences in functional networks of NF1 participants and how these networks respond to cognitive demand of working memory load. We found greater reliance on sensorimotor integration (via postcentral gyrus) in response to working memory. In contrast, NF1 participants had reduced connectivity between higher order networks, which suggests decreased integration of different cognitive processes related to executive control. Additionally, as result of working memory, NF1 participants had weakened connectivity between parts of dorsal attention and control and default mode network, which suggests reduced top-down, goal-directed control.

References

Alahmadi, A. A. S. (2024). Beyond boundaries: investigating shared and divergent connectivity in the pre-/postcentral gyri and supplementary motor area. *NeuroReport*, *35*(5), 283-290. https://doi.org/10.1097/wnr.0000000000002011

Alloway, T. P., Rajendran, G., & Archibald, L. M. D. (2009). Working Memory in Children With Developmental Disorders. *Journal of Learning Disabilities*, *42*(4), 372-382. https://doi.org/10.1177/0022219409335214

Anticevic, A., Cole, M. W., Murray, J. D., Corlett, P. R., Wang, X.-J., & Krystal, J. H. (2012). The role of default network deactivation in cognition and disease. *Trends in Cognitive Sciences*, *16*(12), 584-592. https://doi.org/10.1016/j.tics.2012.10.008

Ashburner, J. (2007). A fast diffeomorphic image registration algorithm. *NeuroImage*, *38*(1), 95-113. https://doi.org/10.1016/j.neuroimage.2007.07.007

Baddeley, A. (2012). Working Memory: Theories, Models, and Controversies. *Annual Review of Psychology*, *63*(1), 1-29. https://doi.org/10.1146/annurev-psych-120710-100422

Behzadi, Y., Restom, K., Liau, J., & Liu, T. T. (2007). A component based noise correction method (CompCor) for BOLD and perfusion based fMRI. *NeuroImage*, *37*(1), 90-101. https://doi.org/10.1016/j.neuroimage.2007.04.042

Boisgueheneuc, F. d., Levy, R., Volle, E., Seassau, M., Duffau, H., Kinkingnehun, S., Samson, Y., Zhang, S., & Dubois, B. (2006). Functions of the left superior frontal gyrus in humans: a lesion study. *Brain*, *129*(12), 3315-3328. https://doi.org/10.1093/brain/awl244

Bruyer, R., & Brysbaert, M. (2011). Combining Speed and Accuracy in Cognitive Psychology: Is the Inverse Efficiency Score (IES) a Better Dependent Variable than

the Mean Reaction Time (RT) and the Percentage Of Errors (PE)? *Psychologica Belgica*, *51*(1). https://doi.org/10.5334/pb-51-1-5

Chan, Y.-S., Jang, J.-T., & Ho, C.-S. (2022). Effects of physical exercise on children with attention deficit hyperactivity disorder. *Biomedical Journal*, *45*(2), 265-270. https://doi.org/10.1016/j.bj.2021.11.011

Cohen, J. R., & D'Esposito, M. (2016). The Segregation and Integration of Distinct Brain Networks and Their Relationship to Cognition. *The Journal of Neuroscience*, *36*(48), 12083-12094. https://doi.org/10.1523/jneurosci.2965-15.2016

Cole, M. W., & Schneider, W. (2007). The cognitive control network: Integrated cortical regions with dissociable functions. *NeuroImage*, *37*(1), 343-360. https://doi.org/10.1016/j.neuroimage.2007.03.071

Corbetta, M., & Shulman, G. L. (2002). Control of goal-directed and stimulus-driven attention in the brain. *Nature Reviews Neuroscience*, *3*(3), 201-215. https://doi.org/10.1038/nrn755

Courtney, S. M., Ungerleider, L. G., Keil, K., & Haxby, J. V. (1997). Transient and sustained activity in a distributed neural system for human working memory. *Nature*, *386*(6625), 608-611. https://doi.org/10.1038/386608a0

Daston, M. M., & Ratner, N. (2005). Neurofibromin, a predominantly neuronal GTPase activating protein in the adult, is ubiquitously expressed during development. *Developmental Dynamics*, *195*(3), 216-226. https://doi.org/10.1002/aja.1001950307

Ding, X., Wu, J., Li, D., & Liu, Z. (2024). The benefit of rhythm-based interventions for individuals with autism spectrum disorder: a systematic review and meta-analysis with random controlled trials. *Frontiers in Psychiatry*, *15*. https://doi.org/10.3389/fpsyt.2024.1436170

Dosenbach, N. U. F., Fair, D. A., Miezin, F. M., Cohen, A. L., Wenger, K. K., Dosenbach, R. A. T., Fox, M. D., Snyder, A. Z., Vincent, J. L., Raichle, M. E., Schlaggar, B. L., & Petersen, S. E. (2007). Distinct brain networks for adaptive and stable task control in humans. *Proceedings of the National Academy of Sciences*, *104*(26), 11073-11078. https://doi.org/10.1073/pnas.0704320104

Eichele, T., Debener, S., Calhoun, V. D., Specht, K., Engel, A. K., Hugdahl, K., von Cramon, D. Y., & Ullsperger, M. (2008). Prediction of human errors by maladaptive changes in event-related brain networks. *Proceedings of the National Academy of Sciences*, *105*(16), 6173-6178. https://doi.org/10.1073/pnas.0708965105

Fisher, R. A. (1915). Frequency Distribution of the Values of the Correlation Coefficient in Samples from an Indefinitely Large Population. *Biometrika*, *10*(4). https://doi.org/10.2307/2331838

Fox, M. D., Snyder, A. Z., Vincent, J. L., Corbetta, M., Van Essen, D. C., & Raichle, M. E. (2005). The human brain is intrinsically organized into dynamic, anticorrelated functional networks. *Proceedings of the National Academy of Sciences*, *102*(27), 9673-9678. https://doi.org/10.1073/pnas.0504136102

Fox, P. T., Burton, H., & Raichle, M. E. (1987). Mapping human somatosensory cortex with positron emission tomography. *Journal of Neurosurgery*, *67*(1), 34-43. https://doi.org/10.3171/jns.1987.67.1.0034

Frank, M. J., Loughry, B., & O'Reilly, R. C. (2001). Interactions between frontal cortex and basal ganglia in working memory: A computational model. *Cognitive, Affective, & Behavioral Neuroscience*, *1*(2), 137-160. https://doi.org/10.3758/cabn.1.2.137

Friston, K. J. (2011). Functional and Effective Connectivity: A Review. *Brain Connectivity*, *1*(1), 13-36. https://doi.org/10.1089/brain.2011.0008

Garg, S., Williams, S., Jung, J., Pobric, G., Nandi, T., Lim, B., Vassallo, G., Green, J., Evans, D. G., Stagg, C. J., Parkes, L. M., & Stivaros, S. (2022). Non-invasive brain

stimulation modulates GABAergic activity in neurofibromatosis 1. *Scientific Reports*, *12*(1). https://doi.org/10.1038/s41598-022-21907-9

Grill-Spector, K., Kourtzi, Z., & Kanwisher, N. (2001). The lateral occipital complex and its role in object recognition. *Vision Research*, *41*(10-11), 1409-1422. https://doi.org/10.1016/s0042-6989(01)00073-6

Groppe, D. M., Urbach, T. P., & Kutas, M. (2011). Mass univariate analysis of event□related brain potentials/fields I: A critical tutorial review. *Psychophysiology*, *48*(12), 1711-1725. https://doi.org/10.1111/j.1469-8986.2011.01273.x

Halai, A. D., Welbourne, S. R., Embleton, K., & Parkes, L. M. (2014). A comparison of dual gradient□echo and spin□echo fMRI of the inferior temporal lobe. *Human Brain Mapping*, *35*(8), 4118-4128. https://doi.org/10.1002/hbm.22463

Ibrahim, A. F. A., Montojo, C. A., Haut, K. M., Karlsgodt, K. H., Hansen, L., Congdon, E., Rosser, T., Bilder, R. M., Silva, A. J., & Bearden, C. E. (2017). Spatial working memory in neurofibromatosis 1: Altered neural activity and functional connectivity. *NeuroImage: Clinical*, *15*, 801-811. https://doi.org/10.1016/j.nicl.2017.06.032

Kirchner, W. K. (1958). Age differences in short-term retention of rapidly changing information. *Journal of Experimental Psychology*, *55*(4), 352-358. https://doi.org/10.1037/h0043688

Kosmas, P., Ioannou, A., & Zaphiris, P. (2018). Implementing embodied learning in the classroom: effects on children's memory and language skills. *Educational Media International*, *56*(1), 59-74. https://doi.org/10.1080/09523987.2018.1547948

Langner, R., Sternkopf, M. A., Kellermann, T. S., Grefkes, C., Kurth, F., Schneider, F., Zilles, K., & Eickhoff, S. B. (2014). Translating working memory into action: Behavioral and neural evidence for using motor representations in encoding visuo-spatial sequences. *Human Brain Mapping*, *35*(7), 3465-3484. https://doi.org/10.1002/hbm.22415

Leech, R., & Smallwood, J. (2019). The posterior cingulate cortex: Insights from structure and function. In *Cingulate Cortex* (pp. 73-85). https://doi.org/10.1016/b978-0-444-64196-0.00005-4

Lehtonen, A., Garg, S., Roberts, S. A., Trump, D., Evans, D. G., Green, J., & Huson, S. M. (2015a). Cognition in children with neurofibromatosis type 1: data from a population-based study. *Developmental Medicine & Child Neurology*, *57*(7), 645-651. https://doi.org/10.1111/dmcn.12734

Lehtonen, A., Garg, S., Roberts, S. A., Trump, D., Evans, D. G., Green, J., & Huson, S. M. (2015b). Cognition in children with neurofibromatosis type 1: data from a population□based study. *Developmental Medicine & Child Neurology*, *57*(7), 645-651. https://doi.org/10.1111/dmcn.12734

Mainy, N., Kahane, P., Minotti, L., Hoffmann, D., Bertrand, O., & Lachaux, J. P. (2007). Neural correlates of consolidation in working memory. *Human Brain Mapping*, *28*(3), 183-193. https://doi.org/10.1002/hbm.20264

Martinussen, R., Hayden, J., Hogg-Johnson, S., & Tannock, R. (2005). A Meta-Analysis of Working Memory Impairments in Children With Attention-Deficit/Hyperactivity Disorder. *Journal of the American Academy of Child & Adolescent Psychiatry*, *44*(4), 377-384. https://doi.org/10.1097/01.chi.0000153228.72591.73

Martuzzi, R., van der Zwaag, W., Farthouat, J., Gruetter, R., & Blanke, O. (2014). Human finger somatotopy in areas 3b, 1, and 2: A 7T fMRI study using a natural stimulus. *Human Brain Mapping*, *35*(1), 213-226. https://doi.org/10.1002/hbm.22172

Marvel, C. L., Morgan, O. P., & Kronemer, S. I. (2019). How the motor system integrates with working memory. *Neuroscience & Biobehavioral Reviews*, *102*, 184-194. https://doi.org/10.1016/j.neubiorev.2019.04.017

Mason, M. F., Norton, M. I., Van Horn, J. D., Wegner, D. M., Grafton, S. T., & Macrae, C. N. (2007). Wandering Minds: The Default Network and Stimulus-Independent Thought. *Science*, *315*(5810), 393-395. https://doi.org/10.1126/science.1131295

Mastria, G., Scaliti, E., Mehring, C., Burdet, E., Becchio, C., Serino, A., & Akselrod, M. (2023). Morphology, Connectivity, and Encoding Features of Tactile and Motor Representations of the Fingers in the Human Precentral and Postcentral Gyrus. *The Journal of Neuroscience*, *43*(9), 1572-1589. https://doi.org/10.1523/jneurosci.1976-21.2022

McNab, F., & Klingberg, T. (2007). Prefrontal cortex and basal ganglia control access to working memory. *Nature Neuroscience*, *11*(1), 103-107. https://doi.org/10.1038/nn2024

Mohr, H. M., Goebel, R., & Linden, D. E. J. (2006). Content- and Task-Specific Dissociations of Frontal Activity during Maintenance and Manipulation in Visual Working Memory. *The Journal of Neuroscience*, *26*(17), 4465-4471. https://doi.org/10.1523/jneurosci.5232-05.2006

Muldoon, S. F., Bridgeford, E. W., & Bassett, D. S. (2016). Small-World Propensity and Weighted Brain Networks. *Scientific Reports*, *6*(1). https://doi.org/10.1038/srep22057

Nee, D. E., Brown, J. W., Askren, M. K., Berman, M. G., Demiralp, E., Krawitz, A., & Jonides, J. (2013). A Meta-analysis of Executive Components of Working Memory. *Cerebral Cortex*, *23*(2), 264-282. https://doi.org/10.1093/cercor/bhs007

Newman, M. E. J. (2006). Modularity and community structure in networks. *Proceedings of the National Academy of Sciences*, *103*(23), 8577-8582. https://doi.org/10.1073/pnas.0601602103

Nieto-Castanon, A. (2020). FMRI denoising pipeline. In *Handbook of functional connectivity Magnetic Resonance Imaging methods in CONN* (pp. 17-25). https://doi.org/10.56441/hilbertpress.2207.6600

North, K., Gutmann, D. H., & International Child Neurology, A. (1997). *Neurofibromatosis type 1 in childhood.*

Onnela, J.-P., Saramäki, J., Kertész, J., & Kaski, K. (2005). Intensity and coherence of motifs in weighted complex networks. *Physical Review E*, *71*(6). https://doi.org/10.1103/PhysRevE.71.065103

Owen, A. M., McMillan, K. M., Laird, A. R., & Bullmore, E. (2005). N□back working memory paradigm: A meta□analysis of normative functional neuroimaging studies. *Human Brain Mapping*, *25*(1), 46-59. https://doi.org/10.1002/hbm.20131

Paulesu, E., Frith, C. D., & Frackowiak, R. S. J. (1993). The neural correlates of the verbal component of working memory. *Nature*, *362*(6418), 342-345. https://doi.org/10.1038/362342a0

Pearson, J., & Keogh, R. (2019). Redefining Visual Working Memory: A Cognitive-Strategy, Brain-Region Approach. *Current Directions in Psychological Science*, *28*(3), 266-273. https://doi.org/10.1177/0963721419835210

Perry, D. W., Zatorre, R. J., Petrides, M., Alivisatos, B., Meyer, E., & Evans, A. C. (1999). Localization of cerebral activity during simple singing. *NeuroReport*, *10*(18), 3979-3984. https://doi.org/10.1097/00001756-199912160-00046

Power, J. D., Barnes, K. A., Snyder, A. Z., Schlaggar, B. L., & Petersen, S. E. (2012). Spurious but systematic correlations in functional connectivity MRI networks arise from subject motion. *NeuroImage*, *59*(3), 2142-2154. https://doi.org/10.1016/j.neuroimage.2011.10.018

Raichle, M. E., MacLeod, A. M., Snyder, A. Z., Powers, W. J., Gusnard, D. A., & Shulman, G. L. (2001). A default mode of brain function. *Proceedings of the National Academy of Sciences*, *98*(2), 676-682. https://doi.org/10.1073/pnas.98.2.676

Ravizza, S. M., Delgado, M. R., Chein, J. M., Becker, J. T., & Fiez, J. A. (2004). Functional dissociations within the inferior parietal cortex in verbal working memory. *NeuroImage*, *22*(2), 562-573. https://doi.org/10.1016/j.neuroimage.2004.01.039

Richter, M. J., Ali, H., & Immink, M. A. (2024). Enhancing Executive Function in Children and Adolescents Through Motor Learning: A Systematic Review. *Journal of Motor Learning and Development*, 1-50. https://doi.org/10.1123/jmld.2024-0038

Rolls, E. T., Huang, C.-C., Lin, C.-P., Feng, J., & Joliot, M. (2020). Automated anatomical labelling atlas 3. *NeuroImage*, *206*. https://doi.org/10.1016/j.neuroimage.2019.116189

Schaefer, A., Kong, R., Gordon, E. M., Laumann, T. O., Zuo, X.-N., Holmes, A. J., Eickhoff, S. B., & Yeo, B. T. T. (2018). Local-Global Parcellation of the Human Cerebral Cortex from Intrinsic Functional Connectivity MRI. *Cerebral Cortex*, *28*(9), 3095-3114. https://doi.org/10.1093/cercor/bhx179

Seeley, W. W., Menon, V., Schatzberg, A. F., Keller, J., Glover, G. H., Kenna, H., Reiss, A. L., & Greicius, M. D. (2007). Dissociable Intrinsic Connectivity Networks for Salience Processing and Executive Control. *The Journal of Neuroscience*, *27*(9), 2349-2356. https://doi.org/10.1523/jneurosci.5587-06.2007

Shilyansky, C., Karlsgodt, K. H., Cummings, D. M., Sidiropoulou, K., Hardt, M., James, A. S., Ehninger, D., Bearden, C. E., Poirazi, P., Jentsch, J. D., Cannon, T. D., Levine, M. S., & Silva, A. J. (2010). Neurofibromin regulates corticostriatal inhibitory networks during working memory performance. *Proceedings of the National Academy of Sciences*, *107*(29), 13141-13146. https://doi.org/10.1073/pnas.1004829107

Shine, James M., Bissett, Patrick G., Bell, Peter T., Koyejo, O., Balsters, Joshua H., Gorgolewski, Krzysztof J., Moodie, Craig A., & Poldrack, Russell A. (2016). The Dynamics of Functional Brain Networks: Integrated Network States during Cognitive Task Performance. *Neuron*, *92*(2), 544-554. https://doi.org/10.1016/j.neuron.2016.09.018

Simmonds, D., Fotedar, S., Suskauer, S., Pekar, J., Denckla, M., & Mostofsky, S. (2007). Functional brain correlates of response time variability in children. *Neuropsychologia*, *45*(9), 2147-2157. https://doi.org/10.1016/j.neuropsychologia.2007.01.013

Simons, J. S., & Spiers, H. J. (2003). Prefrontal and medial temporal lobe interactions in long-term memory. *Nature Reviews Neuroscience*, *4*(8), 637-648. https://doi.org/10.1038/nrn1178

Spadone, S., Della Penna, S., Sestieri, C., Betti, V., Tosoni, A., Perrucci, M. G., Romani, G. L., & Corbetta, M. (2015). Dynamic reorganization of human resting-state networks during visuospatial attention. *Proceedings of the National Academy of Sciences*, *112*(26), 8112-8117. https://doi.org/10.1073/pnas.1415439112

Srinivasan, S. M., Eigsti, I.-M., Gifford, T., & Bhat, A. N. (2016). The effects of embodied rhythm and robotic interventions on the spontaneous and responsive verbal communication skills of children with Autism Spectrum Disorder (ASD): A further outcome of a pilot randomized controlled trial. *Research in Autism Spectrum Disorders*, *27*, 73-87. https://doi.org/10.1016/j.rasd.2016.04.001

Swanson, H. L., & Alloway, T. P. (2012). Working memory, learning, and academic achievement. In *APA educational psychology handbook, Vol 1: Theories, constructs, and critical issues*. (pp. 327-366). https://doi.org/10.1037/13273-012

Thomas Yeo, B. T., Krienen, F. M., Sepulcre, J., Sabuncu, M. R., Lashkari, D., Hollinshead, M., Roffman, J. L., Smoller, J. W., Zöllei, L., Polimeni, J. R., Fischl, B., Liu, H., & Buckner, R. L. (2011). The organization of the human cerebral cortex estimated by intrinsic functional connectivity. *Journal of Neurophysiology*, *106*(3), 1125-1165. https://doi.org/10.1152/jn.00338.2011

Todd, J. J., & Marois, R. (2004). Capacity limit of visual short-term memory in human posterior parietal cortex. *Nature*, *428*(6984), 751-754. https://doi.org/10.1038/nature02466

Tomporowski, P. D., Davis, C. L., Miller, P. H., & Naglieri, J. A. (2007). Exercise and Children's Intelligence, Cognition, and Academic Achievement. *Educational Psychology Review*, *20*(2), 111-131. https://doi.org/10.1007/s10648-007-9057-0

Tomson, S. N., Schreiner, M. J., Narayan, M., Rosser, T., Enrique, N., Silva, A. J., Allen, G. I., Bookheimer, S. Y., & Bearden, C. E. (2015). Resting state functional MRI reveals abnormal network connectivity in neurofibromatosis 1. *Human Brain Mapping*, *36*(11), 4566-4581. https://doi.org/10.1002/hbm.22937

Uddin, L. Q. (2014). Salience processing and insular cortical function and dysfunction. *Nature Reviews Neuroscience*, *16*(1), 55-61. https://doi.org/10.1038/nrn3857

Violante, I. R., Ribeiro, M. J., Cunha, G., Bernardino, I., Duarte, J. V., Ramos, F., Saraiva, J., Silva, E., & Castelo-Branco, M. (2012). Abnormal Brain Activation in Neurofibromatosis Type 1: A Link between Visual Processing and the Default Mode Network. *PLoS ONE*, *7*(6). https://doi.org/10.1371/journal.pone.0038785

Violante, I. R., Ribeiro, M. J., Edden, R. A. E., Guimarães, P., Bernardino, I., Rebola, J., Cunha, G., Silva, E., & Castelo-Branco, M. (2013). GABA deficit in the visual cortex of patients with neurofibromatosis type 1: genotype–phenotype correlations and functional impact. *Brain*, *136*(3), 918-925. https://doi.org/10.1093/brain/aws368

Wang, Y., Zhang, Y.-b., Liu, L.-l., Cui, J.-f., Wang, J., Shum, D. H. K., van Amelsvoort, T., & Chan, R. C. K. (2017). A Meta-Analysis of Working Memory Impairments in Autism Spectrum Disorders. *Neuropsychology Review*, *27*(1), 46-61. https://doi.org/10.1007/s11065-016-9336-y

Whitfield-Gabrieli, S., & Nieto-Castanon, A. (2012). Conn: A Functional Connectivity Toolbox for Correlated and Anticorrelated Brain Networks. *Brain Connectivity*, *2*(3), 125-141. https://doi.org/10.1089/brain.2012.0073

Xia, M., Wang, J., & He, Y. (2013). BrainNet Viewer: A Network Visualization Tool for Human Brain Connectomics. *PLoS ONE*, *8*(7). https://doi.org/10.1371/journal.pone.0068910

Yamashita, M., Yoshihara, Y., Hashimoto, R., Yahata, N., Ichikawa, N., Sakai, Y., Yamada, T., Matsukawa, N., Okada, G., Tanaka, S. C., Kasai, K., Kato, N., Okamoto, Y., Seymour, B., Takahashi, H., Kawato, M., & Imamizu, H. (2018). A prediction model of working memory across health and psychiatric disease using whole-brain functional connectivity. *eLife*, *7*. https://doi.org/10.7554/eLife.38844

Zalesky, A., Fornito, A., & Bullmore, E. T. (2010). Network-based statistic: Identifying differences in brain networks. *NeuroImage*, *53*(4), 1197-1207. https://doi.org/10.1016/j.neuroimage.2010.06.041